CrystEngComm

RSC Publishing

PAPER

View Article Online
View Journal | View Issue

Cite this: *CrystEngComm*, 2013, **15**, 2466

Can a single pyridinedicarboxylic acid be ample enough to nucleate supramolecular double helices in enantiomeric pseudopeptides?†‡

Anita Dutt Konar*

Received 24th November 2012,
Accepted 12th January 2013

DOI: 10.1039/c3ce26912d

www.rsc.org/crystengcomm

Two enantiomeric pseudopeptides **I** & **II**, comprising a single pyridinedicarboxylic acid and a flexible dipeptidyl fragment H-Xaa-*m*ABA-OMe (Xaa: L-Ala, pseudopeptide **I**; D-Ala, pseudopeptide **II**, *m*ABA: *meta* aminobenzoic acid), have been synthesized using Boc chemistry. X-ray crystallographic analysis reveals that in the solid state, both the enantiomers form a dimeric unit stabilized by intermolecular hydrogen bonding interactions. Interestingly, these dimeric subunits self-assemble to form a supramolecular double helical architecture using various noncovalent interactions. To date, significant examples are documented in the literature where DNA analogues/derivatives or several rigid templates have been employed as synthons for double helical self assembly. However, to the best of our knowledge, this novel example represents one of the very few reports of a supramolecular double helix design resulting from the self assembly of a flexible dimeric peptidyl unit, solely nucleated by the conformational features, of the peptides. Concentration and temperature dependant NMR experiments were performed for pseudopeptide **I** (one of the enantiomers) to decipher the existence of the dimeric unit in solution. Pseudopeptide **II** (one of the enantiomers) was subjected to iodine and gas absorption studies, which demonstrates its candidature in the design of nanoporous materials.

Introduction

The mimicry of helical entities into double or triple strands has emerged as a focal point of bioorganic and medicinal chemistry.[1] Since the inspirational discovery of the DNA double helix by Watson and Crick in natural systems, chemists have been motivated to design hybridization patterns that possess the ability to intertwine into multiple helices.[2] Over the past few years, considerable progress has been devised in stabilizing dimeric ensembles, mainly from DNA analogues or their derivatives.[3] However, the design of non-DNA moieties as synthons for supramolecular double helix formations is much less evolved and is of current research interest to the scientific community.[4] In this context, Yashima and his co-workers are extensively recognized for their contribution to double helix stabilization by intermolecular salt-bridge formations[5] and π–π interactions.[6] The twisting of supramolecular polymeric ladders reported by Sada and his group represents another approach of nucleating double helical assembly.[7] Gabriel and Iverson are known for their substantial input into double helical stabilization by alternating the stacking of electron rich and electron poor aromatic systems.[8] The double helical stabilization by a self-complementary array of hydrogen bond donors and acceptors by Wisner and his group is noteworthy.[9] Apart from these, the design of artificial oligoamides constitutes another class of synthons in supramolecular double helix stabilization. In this context, the pioneering contribution of Lehn and his co-workers in studying the dynamic exchange of aromatic oligoamides into single and double stranded helicates needs special mention.[10] A careful search shows that Huc and his group have made novel contributions in the design of supramolecular double helices using several aromatic heterocycles or their derivatives.[11]

As part of the investigation into determining the motifs for supramolecular double helix stabilization from suitable building blocks, this project aims to utilize a single pyridinyl unit *i.e.* 2,6 pyridinedicarboxylic acid coupled with H-Xaa-*m*ABA-OMe (where Xaa is L-Ala, Peptide **I**; D-Ala, Peptide **II**) using Boc chemistry (Fig. 1). The design of the double helical complex was approached based on the hydrogen bonding interaction between a planar six-membered heterocycle containing nitrogen based donor/acceptor groups that are connected sequentially in a 1,3 manner (pyridine). As a further design element, a simple dipeptidyl sequence, comprising

Dept of Chemical Sciences, Indian Institute of Science Education and Research, Bhopal, ITI Gas Rahat Building, Govindpura, Bhopal 462023, India.
E-mail: anita@iiserb.ac.in; Fax: +91 7554092392; Tel: +91 7554056278

† Dedicated to Professor Animesh Pramanik, University of Calcutta, for his significant contribution in the field of peptidomimetics.

‡ Electronic supplementary information (ESI) available: NMR, mass and CIF files of peptides **I** and **II** respectively. CCDC 894165 and 894166. For ESI and crystallographic data in CIF or other electronic format see DOI: 10.1039/c3ce26912d

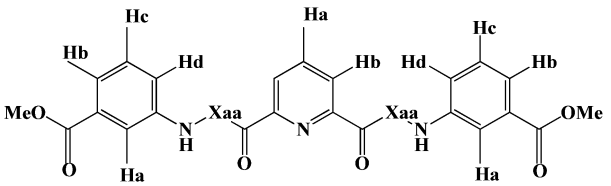

Xaa = L-Ala, Pseudopeptide **I**

Xaa = D-Ala, Pseudopeptide **II**

Fig. 1 Schematic representation of pseudopeptides **I** & **II**.

naturally occurring amino acids and conformationally biased *meta* amino benzoic acid (*: although pseudopeptides **I** and **II** are enantiomers, their different chemical formula in Table 1 reflects the presence of disordered solvent molecules which we are unable to resolve) having β-sheet forming propensity, was chosen.[12] The idea was to decipher whether the dipeptidyl fragments present in enantiomeric pseudopeptides **I** and **II** are ample enough to nucleate double helical assembly when coupled to a single pyridine 2,6 dicarboxylic acid unit. Concentration and temperature dependant NMR experiments were performed for pseudopeptide **I** (one of the enantiomers) to decipher the existence of the dimeric unit in solution.

Pseudopeptides **II** (one of the enantiomers) was subjected to iodine and gas adsorption studies to explore its candidature in the design of nanoporous materials.

Experimental

Abbreviations

Aib, α-aminoisobutyric acid; TFA, trifluoroacetic acid; *m*ABA, *m*-amino benzoic acid; Boc, tertiary butyloxy carbonyl; OMe, methoxy carbonyl; DCC, dicyclohexylcarbodiimide; HOBt, 1-hydroxy benzotriazole.

Table 1 Crystallographic refinement details for pseudopeptides **I** and **II**

	Pseudopeptide **I**	Pseudopeptide **II**
Chemical formula*	$2(C_{29}\ H_{29}N_5\ O_8),C_2O$	$2(C_{29}\ H_{29}N_5\ O_8),C_4O$
Formula weight (g)	1191.16	1215.18
Crystal system	Tetragonal	Tetragonal
Space group	*P*41212	*P*43212
a (Å)	13.627(4)	13.5368(6)
b (Å)	13.627(4)	13.5368(6)
c (Å)	36.416(12)	36.4665(15)
$\alpha(^\circ)$	90	90
$\beta\ (^\circ)$	90	90
$\gamma\ (^\circ)$	90	90
$V\ (Å^3)$	6763(4)	6682.3(5)
Z	4	4
Collected reflections	7129	7415
Unique reflections	3099	5753
γ (Mo–Kα)(Å)	0.71073	0.71073
T (K)	296(2)	296(2)
R_1	0.0907	0.0717
$wR_2[I > 2\sigma(I)]$	0.2331	0.2208

Synthesis of the peptides

Pseudopeptides **I** & **II** containing two terminal methoxy carbonyls were synthesized using conventional solution phase methodology, with racemization free techniques, followed by a fragment condensation strategy (Scheme 1).[13] The *t*-butyloxycarbonyl and methyl ester groups were used for the amino and carboxyl protections respectively and dicyclohexylcarbodiimide (DCC) and 1-hydroxy benzotriazole (HOBT) were used as coupling agents for the synthesis of the dipeptides. Methyl ester hydrochlorides of *m*ABA were prepared by the thionyl chloride–methanol procedure.[12] All the intermediates obtained were checked for purity by thin layer chromatography (TLC) on silica gel and used without further purification. All the final pseudopeptides were purified by column chromatography using silica gel (100–200 mesh) as the stationary phase and ethyl acetate and petroleum ether mixture as the eluent. The reported pseudopeptides **I** & **II** were fully characterised by X-ray crystallography, NMR and mass spectrometry.

Boc-L-Ala-*m*ABA-OMe (1). Ref. 12*b*.

Boc-D-Ala-*m*ABA-OMe (2). The methyl *m*-aminobenzoate (1.52 g, 10 mmol), obtained from its hydrochloride (3.76, 20 mmol) was added to an ice-cool solution of Boc-D-Ala-OH (1.9 g, 10 mmol) in 10 ml of DCM. Then DCC (2 g, 10 mmol; 1,3-dicyclohexylcarbodiimide) was added to the cooled mixture, which was stirred for a day at room temperature. The residue was then added into ethyl acetate (50 ml) and the DCU (*N*,*N*-dicyclohexylurea) was filtered off. The organic layer was washed with 2 M HCl (3 × 50 ml), 1 M sodium carbonate (3 × 50 ml) and brine (2 × 50 ml), dried over anhydrous sodium sulfate and evaporated *in vacuo* to yield a solid material. The crude peptide was used without further purification.

Yield: 2.98 g (9.22 mmol, 92%). Mp: 145°; ^{1}H NMR 400 MHz ($CDCl_3$; δ ppm): 1.24–1.25 (3H, d), 1.45 (9H, s), 3.85 (3H, s), 4.43–4.47 (1H, m), 5.42–5.60 (1H, m), 7.62–8.10 (4-Ar–Hs), 9.14–9.16 (1H, m); ^{13}C NMR 100 MHz ($CDCl_3$; δ ppm): 17.8, 28.6, 50.2, 52, 80.4, 120.7, 124.1, 125.3, 128.9, 130.7, 138.2, 156, 167, 172.1.

Peptide I. Trifluoroacetic acid (5 ml) was added to Boc-L-Ala-*m*ABA-OMe (**1**) (1.5 g, 4.65 mmol) at 0 °C and stirred at room temperature. The removal of the Boc group was monitored by TLC. After 6 hours, the trifluoroacetic acid was removed under reduced pressure to afford the crude trifluoroacetate salt. The residue was taken up in water and washed with diethyl ether. The pH of the aqueous solution was adjusted to pH 8 with

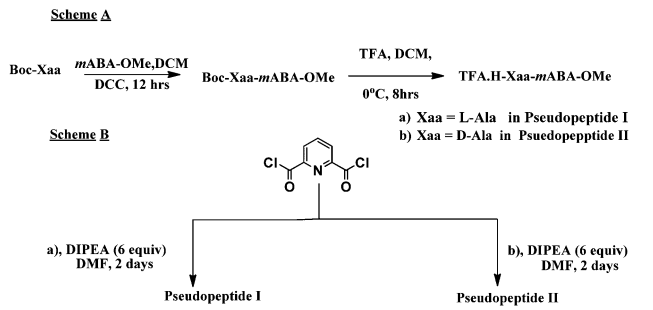

Scheme 1 Synthetic strategy of pseudopeptide **I** and **II**.

sodium bicarbonate and extracted with ethyl acetate. The extracts were pooled, washed with saturated brine, dried over sodium sulphate and concentrated to a highly viscous liquid that gave a positive ninhydrin test. DMF and DIPEA (3.2 ml, 13.98 mmol) was added to a well stirred and ice-cooled solution of the obtained free base. To this mixture, a freshly prepared solution of pyridine 2,6 dicarbonyldichloride (0.44 g, 2.33 mmol) in 10 ml of DMF was added over a period of 0.5 hours and the mixture continued to stir at room temperature for 2 days. The solvents were evaporated *in vacuo*, the residue was dissolved in ethyl acetate and washed sequentially with 1 M HCl (3 × 30 ml), a 1 M Na_2CO_3 solution (3 × 30 ml) and again with water. The solvent was then dried over anhydrous Na_2SO_4 and evaporated *in vacuo*, giving a light yellow solid. Purification was done using silica gel as the stationary phase and an ethyl acetate–petroleum ether mixture as the eluent. Single crystals were grown from an acetone–petroleum ether mixture (90 : 10) by slow evaporation and were stable at room temperature.

Yield: 0.65 g (50.0%, 1.16 mmol). Mp = 192–193 °C; IR (KBr): 1292, 1442, 1540, 1655, 1724, 3291 cm^{-1}; ^1H NMR 400 MHz ($CDCl_3$, δ ppm): 1.66 (6H, d, J = 8 Hz, Ala(1) $C^{\beta}Hs$), 3.89 (6H, s, methoxy H's), 4.93–4.98 (2H, m, Ala(1) $C^{\alpha}Hs$), 7.34 (2H, t, J = 8 Hz, Hc (*m*-ABA(2)), 7.74 (2H, d, J = 8 Hz, Hb (*m*-ABA(2)), 7.95 (2H, d, J = 8 Hz, Hd (*m*-ABA(2)), 8.04 (1H, t, J = 8 Hz, py Ha), 8.12 (2H, s, Ha (*m*-ABA(2)), 8.37 (1H, d, J = 8 Hz, py Hb), 8.9 (2H, d, J = 8 Hz, Ala(1) NH), 9.2 (2H, s, *m*ABA(2) NH); ^{13}C NMR 100 MHz($CDCl_3$, δ ppm): 17.8, 50.2, 52.2, 120.9, 124.4, 125.3, 125.5, 129.0, 130.7, 138.2, 139.2, 148.4, 164.01, 166.71, 171.11; HR–MS $C_{29}H_{29}N_5O_8$ $(M + Na^+)$ = 598.195, M_{calcd} $C_{29}H_{29}N_5O_8$ $(M + Na)^+$ = 598, $C_{58}H_{58}N_{10}O_{16}$ $(M + Na^+)$ = 1173.3736, M_{calcd} $C_{29}H_{29}N_5O_8$ $(M + Na)^+$ = 1173.

Peptide II. Trifluoroacetic acid (5 ml) was added to Boc-D-Ala-*m*ABA-OMe (**2**) (1.5 g, 4.65 mmol) at 0 °C and stirred at room temperature. The removal of the Boc group was monitored by TLC. After 6 hours, the trifluoroacetic acid was removed under reduced pressure to afford the crude trifluoroacetate salt. The residue was taken up in water and washed with diethyl ether. The pH of the aqueous solution was adjusted to pH 8 with sodium bicarbonate and extracted with ethyl acetate. The extracts were pooled, washed with saturated brine, dried over sodium sulphate and concentrated to a highly viscous liquid that gave a positive ninhydrin test. DMF and DIPEA (3.2 ml, 13.98 mmol) was added to a well stirred and ice-cooled solution of the obtained free base. To this mixture, a freshly prepared solution of pyridine 2,6 dicarbonyl dichloride (0.44 g, 2.33 mmol) in 10 ml of DMF was added over a period of 0.5 hours and the mixture continued to stir at room temperature for 2 days. The solvents were evaporated *in vacuo* and the residue was dissolved in ethyl acetate and washed sequentially with 1 M HCl (3 × 30 ml), a 1 M Na_2CO_3 solution (3 × 30 ml) and again with water. The solvent was then dried over anhydrous Na_2SO_4 and evaporated *in vacuo*, giving a light yellow solid. Purification was done using silica gel as the stationary phase and an ethyl acetate–petroleum ether mixture as the eluent. Single crystals were grown from an acetone–petroleum ether mixture (90 : 10) by slow evaporation and were stable at room temperature.

Yield: 0.52 g (40.0%, 0.93 mmol). Mp = 150–152 °C; IR (KBr): 1273, 1400, 1531, 1672, 1723, 3436 cm^{-1}; ^1H NMR 400 MHz ($CDCl_3$, δ ppm): 1.62–1.63 (6H, m, Ala(1) $C^{\beta}Hs$), 3.93 (6H, s, methoxy H's), 4.58–4.62 (2H, m, Ala(1) $C^{\alpha}Hs$), 7.42–7.43 (1H, m, Hc (*m*-ABA(2)), 7.82 (2H, d, J = 4 Hz, Hb (*m*-ABA(2)), 7.91 (2H, d, J = 4 Hz, Hd (*m*-ABA(2)), 8.12–8.09 (1H, m, py Ha), 8.14 (2H, s, Ha (*m*-ABA(2)), 8.27 (2H, s, py Hb), 8.40 (2H, d, J = 8 Hz, Ala(1) NH), 8.75 (2H, d, J = 8 Hz, *m*ABA(2)NH); ^{13}C NMR 100 MHz ($CDCl_3$, δ ppm): 17.7, 50.2, 52.2, 120.9, 124.4, 125.4, 125.5, 129.1, 130.7, 138.2, 139.2, 148.4, 164, 166.7, 170.9,; HR–MS $C_{29}H_{29}N_5O_8$ $(M + Na^+)$ = 598.197, M_{calcd} $C_{29}H_{29}N_5O_8$ $(M + Na)^+$ = 598, $C_{58}H_{58}N_{10}O_{16}$ $(M + Na^+)$ = 1173.3756, M_{calcd} $C_{29}H_{29}N_5O_8$ $(M + Na)^+$ = 1173.

X-ray crystallography

Data collection of the compounds was performed at 296 K on a Bruker Apex II diffractometer with Mo–Kα (λ = 0.71073 Å) radiation. Data reduction and cell refinement were performed with the SAINT program and the absorption correction program SADABS[14] was employed to correct the data for absorption effects. The crystal structures were solved by direct methods and refined with full-matrix least-squares (SHELXTL-97)[15] with atomic coordinates and anisotropic thermal parameters for non-hydrogen atoms. The atoms of the disordered solvent molecules were refined isotropically. As the quality of the crystals was poor, the data obtained was also poor, which finally resulted in large ADP values for some non-solvent hydrogen atoms in **1**. Higher experimental temperatures (296 K) could be another reason for this. The crystallographic data are summarized in Table 1. The SHELXTL, Mercury and Diamond software were used to visualize the structures.

Gas adsorption studies

N_2 absorption studies at 77 K with dehydrated samples prepared at 373 K under a high vacuum were carried out using a fully computer-controlled volumetric Belsorp-Max surface area analyzer. The nitrogen gas used for the measurements was of scientific/research grade with 99.999% purity. The dead volume of the sample cell was measured using helium gas of 99.999% purity. Non-ideal corrections were made by applying virial coefficients at the measurement temperature.

Results and discussion

Solid state conformational analysis

Single crystals suitable for X-ray diffraction were obtained from a mixture of acetone and petroleum ether after slow evaporation. Both the enantiomeric pseudopeptides **I** and **II** crystallize with one molecule in the asymmetric unit. The crystallographic parameters for both the pseudopeptides are reported in Table 1.

The solid state structure of enantiomeric pseudopeptides **I** and **II** reveal a bent conformation near the central aromatic system and an overall extended structure around the dipeptidyl fragment, where the aromatic units are in edge-to-face and

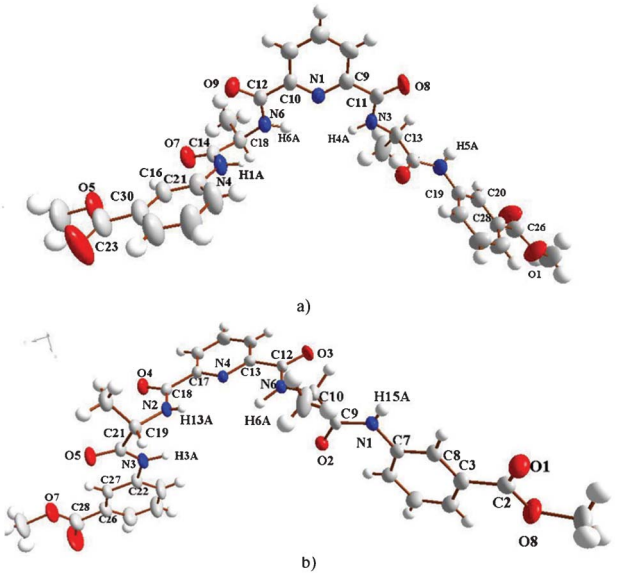

Fig. 2 Crystal Structure of (a) pseudopeptide **I** (b) pseudopeptide **II** with an atom numbering scheme.

face-to-face contact with the central pyridine ring (Fig. 2). The torsion angles and hydrogen bonding parameters of both the pseudopeptides are presented in Table 2 and 3 respectively. Each molecule of pseudopeptide **I** and **II** first forms a dimeric entity (molecule 1 and 2 of the same pseudopeptide; molecule 1 is shown as a capped stick and molecule 2 as a ball and stick), where the two central pyridine rings slightly interdigitate with each other and the two arms of the dipeptidyl fragment are in a mirror image relationship connected by two intermolecular hydrogen bonds (Fig. 3a: pseudopeptide **I**, Fig. 4a: pseudopeptide **II**). In pseudopeptide **I**, the molecule 1pyridinyl CO forms a hydrogen bond with the molecule 2

Table 2 Selected torsion angles (°) for pseudopeptides **I** and **II**

Pseudopeptide **I**			
C10–N1–C9–C11	177.8(5)	C9–N1–C10–C12	−179.5(5)
N1–C9–C11–N3	2.9(7)	N1–C10–C12–N6	0.3(7)
C9–C11–N3–C13	173.2(5)	C10–C12–N6–C18	−173.2(4)
C11–N3–C13–C8	88.4(6)	C12–N6–C18–C14	−59.8(6)
N3–C13–C8–N2	−162.5(4)	N6–C18–C14–N4	−30.2(6)
C13–C8–N2–C19	−165.7(4)	C18–C14–N4–C21	−173.8(5)
C8–N2–C19–C20	161.1(5)	C14–N4–C21–C16	−3.7(9)
N2–C19–C20–C28	180.0(5)	N4–C21–C16–C30	−179.5(5)
C19–C20–C28–C26	176.7(5)	C21–C16–C30–C23	−178.7(6)
C20–C28–C26–O1	171.8(6)	C16–C30–C23–C30	−7(1)
Pseudopeptide **II**			
C17–N4–C13–C12	−178.4(3)	C13–N4–C17–C18	−179.8(3)
N4–C13–C12–N6	−2.9(4)	N4–C17–C18–N2	0.2(4)
C13–C12–N6–C10	−174.6(3)	C17–C18–N2–C19	172.1(3)
C12–N6–C10–C9	−88.2(4)	C18–N2–C19 –C21	60.2(4)
N6–C10–C9–N1	163.1(3)	N2–C19 –C21–N3	29.9(4)
C10–C9–N1–C7	167.0(3)	C19 –C21–N3–C22	174.6(3)
C9–N1–C7–C8	−160.3(3)	C21–N3–C22–C27	2.4(5)
N1–C7–C8–C3	179.2(3)	N3–C22–C27–C26	−178.0(8)
C7–C8–C3–C2	−176.1(3)	C22–C27–C26–C28	177.9(4)
C8–C3–C2–O8	−173.5(3)	C27–C26–C28–O7	6.7(6)

Table 3 Intermolecular hydrogen bonding parameters of pseudopeptides **I** and **II**

D–H···A	H···A/Å	D···A/Å	D–H···A/°
Pseudopeptide **I**			
N3–H4A···O3[a]	2.13	2.95	155.2
N4–H1A···O8[a]	2.18	3.00	160.5
N2–H5A···O9[a]	2.02	2.87	162.7
Pseudopeptide **II**			
N1–H15A···O4[a]	2.24	2.86	163.5
N3–H3A···O3[a]	2.08	2.99	155.4
N6–H6A···O2[a]	1.97	2.95	156.8

[a] Symmetry equivalent *x*, *y*, *z*.

*m*ABA NH (N4–H1A···O8, 2.18 Å; N4···O8, 3.00 Å; N4–H1A···O8 160.5°; *x*, *y*, *z*) and molecule 1 Ala NH forms a hydrogen bond to molecule 2 Ala CO (N3–H4A···O3, 2.13 Å, N3···O3, 2.95 Å, N3–H4A···O3, 155.2°, *x*, *y*, *z*), to stabilize the dimeric structure (Table 3). A similar type of dimeric moiety is also formed by two molecules of the enantiomeric pseudopeptide **II** (N3–H3A···O3, 2.08 Å, N3···O3, 2.99 Å, N3–H3A···O3 155.37°, *x*, *y*, *z*); (N6–H6A···O2, 1.97 Å, N6···O2, 2.95 Å, N6–H6A···O2, 156.83°, *x*, *y*, *z*) (Table 3). The crystal structure of both the pseudopeptides reveal the presence of a C_2 symmetric axis.

Interestingly, each dimeric entity of the enantiomeric pseudopeptides **I** and **II** are then regularly stacked one on top of the other, maintaining a proper registry to form an intermolecular hydrogen bonded helical strand along the crystallographic *a*-axis.

There is a single intermolecular hydrogen bond between molecule 1 *m*ABA NH and molecule 2 pyridinyl CO of another dimeric set (N2–H5A···O9, 2.09 Å N2···O9, 2.87 Å, N2–H5A···O9, 162.7°, *x*, *y*, *z* for peptide **I** and N1–H15A···O4, 2.24 Å, N1···O4, 2.86 Å, N1–H15A···O4, 163.5°; *x*, *y*, *z* peptide **II**, Table 3) (Fig. 3b

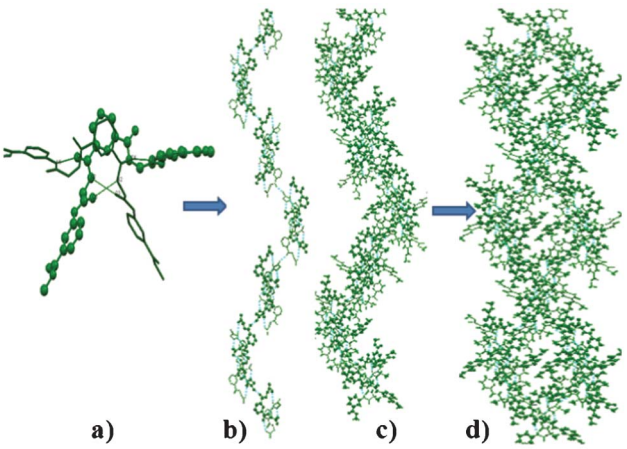

Fig. 3 Schematic representation of the stepwise supramolecular double helix formation from pseudopeptide **I** a) Dimeric entity; Single helical strand b) without sidechains and nonhydrogen bonded atoms; c) with sidechains and all atoms; d) double helical assembly along the crystallographic *a*-axis. (Hydrogen bonded atoms are shown as dotted lines.)

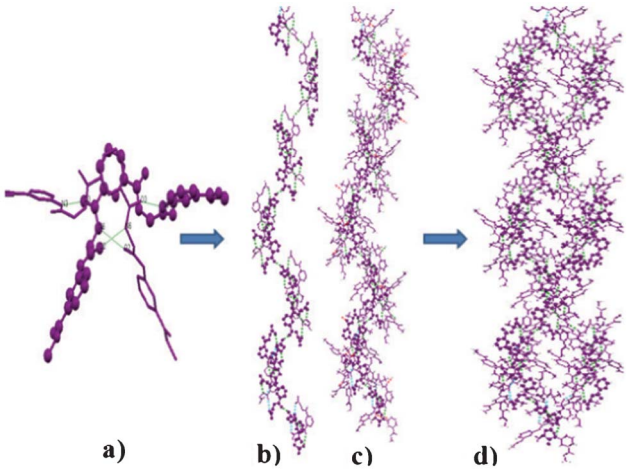

Fig. 4 Schematic representation of the stepwise supramolecular double helix formation from pseudopeptide **II** a) Dimeric entity; Single helical strand b) without sidechains and nonhydrogen bonded atoms; c) with sidechains and all atoms; d) double helical assembly along the crystallographic *a*-axis. (Hydrogen bonded atoms are shown as dotted lines.)

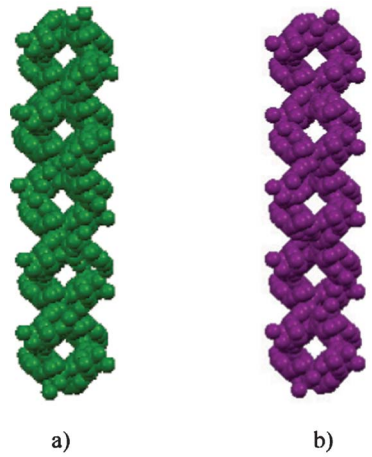

Fig. 5 The formation of the supramolecular double helical assembly of a) pseudopeptide **I** and b) pseudopeptide **II**, as observed along the crystallographic *c*-axis in a spacefilling model.

and 4b) which is responsible for creating a single strand of the double helix along the crystallographic *a*-axis, respectively.

These individual helical strands are then tethered *via* non-covalent interactions to form the supramolecular double

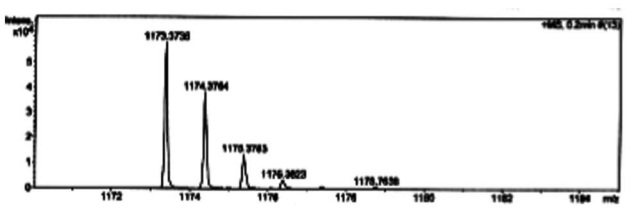

Fig. 6 Mass spectra of pseudopeptide **I**.

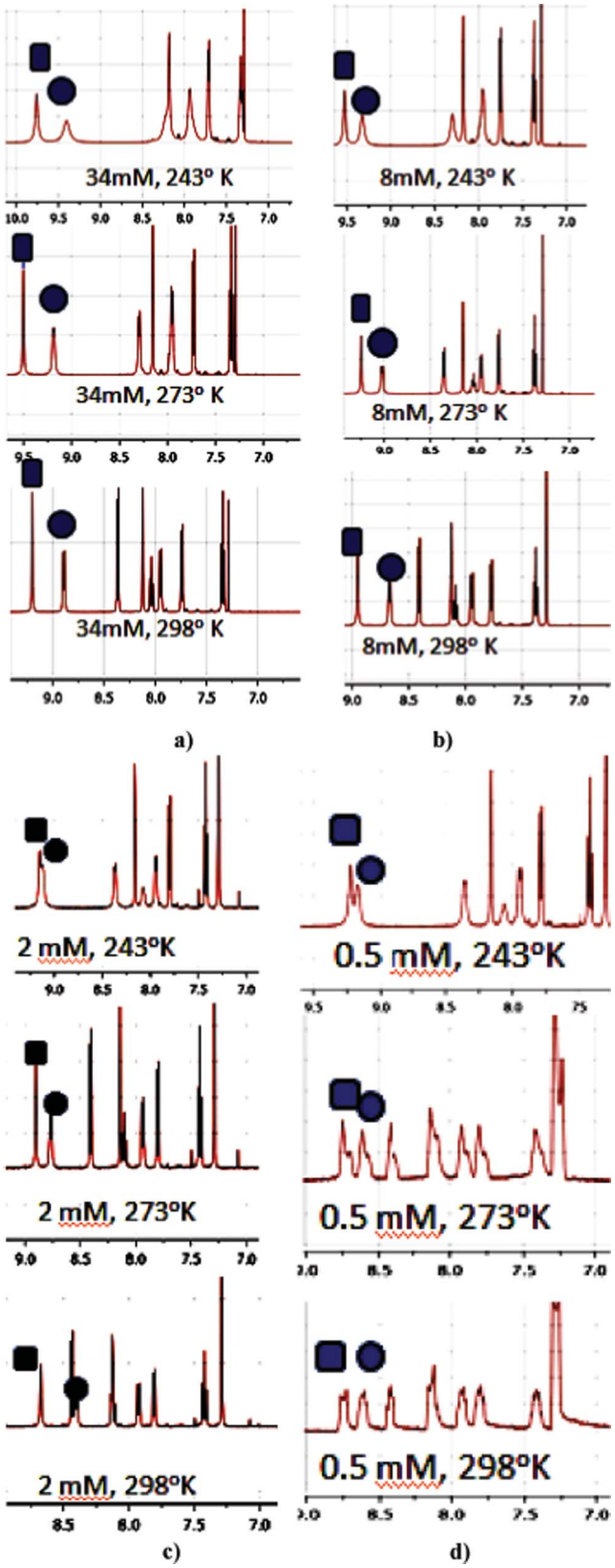

Fig. 7 500 MHz ^{1}H NMR spectra of (aromatic and NH region) pseudopeptide **I** a) 34 mM; b) 8 mM; c) 2 mM; d) 0.5 mM in $CDCl_3$ at different temperatures. Ala(1) NH (round) and *m*ABA(2) NH are marked as rounded squares.

helical superstructure along the crystallographic *a*-axis (Fig. 3c and 4c). The torsion angle around the central pyridinyl moiety plays a crucial role in dictating the overall double helical structural features. Fig. 3 and 4 represents a schematic diagram of the stepwise formation of the supramolecular double helix starting from the dipeptidyl building blocks as subunits for both the pseudopeptides. Fig. 5 also depicts a clear view of the supramolecular double helical assemblage of both the enantiomeric pseudopeptides **I** and **II**, respectively in a spacefilled model, as is observed along the crystallographic *c*-axis. It is interesting to note that the *m*ABA units present in each duplex are engaged in multiple intraduplex interstrand face-to-face and edge-to-face interactions at various angles, which may be responsible for the overall stabilization of these motifs.

Solution conformational analysis

In order to explore the solution conformational features of enantiomeric pseudopeptides **I** and **II**, ESI-MS and NMR studies were performed. The enantiomeric pseudopeptides **I** and **II** reveal signals of *m*/*z* 2M + Na (**I**:1173.3736; **II**:1173.3956) in the ESI-MS analysis (Fig. 6), supporting the formation of dimers in MeOH.[16] However, the relative signal intensities do not simply reflect the relative amounts of the species in solution as it is affected by many experimental parameters. Therefore, concentration and temperature dependant NMR studies in $CDCl_3$ were carried out to substantiate the MS results.

The spectra of the pseudopeptides were recorded at several concentrations and temperatures. A comparison of the proton chemical shifts of pseudopeptide **I** in concentrated and dilute solutions is presented in Fig. 7. The NMR analysis reveals that at a particular concentration, the amide protons of alanine and *meta* amino benzoic acid moieties exhibit higher resonance frequencies with a decrease in the temperature, which may be attributed to the hydrogen-bonding interactions predicted in the dimeric assembly. Conversely, all the aromatic protons shift upfield as a consequence of the π–π interactions and ring currents exerted by them. In order to determine whether the hydrogen bonds are intra or intermolecular, dilution experiments were performed.[17] The NH resonances reveal considerable shifts with a change in concentration, suggesting the presence of intermolecular hydrogen bonding within the pseudopeptides. Had it been intramolecular, there would be a negligible change in their chemical shifts with

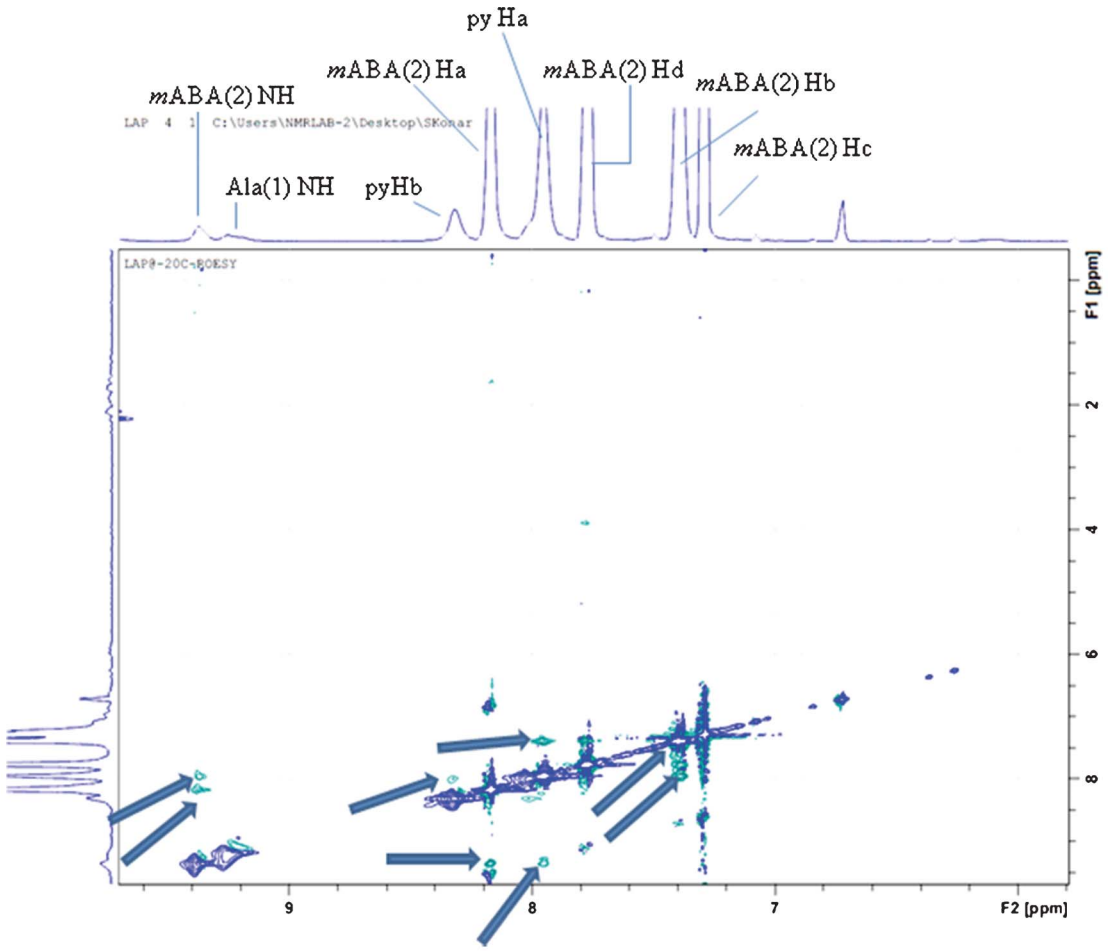

Fig. 8 500 MHz ROESY spectrum of pseudopeptide **I** in $CDCl_3$ exhibiting the NOE intensities responsible for the intermolecular hydrogen bonding interactions between the aromatic and NH protons (marked with arrows).

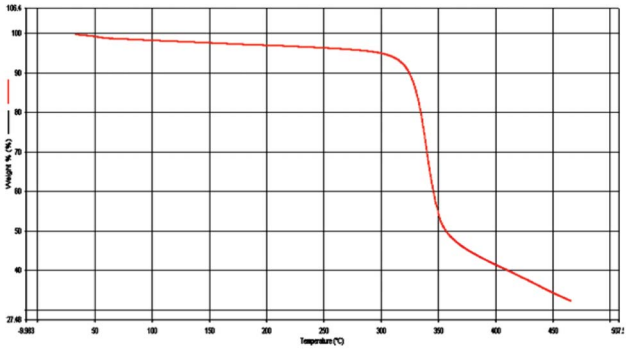

Fig. 9 TGA of pseudopeptide **II**. (It is evident that the compound exhibits no decomposition, phase transition or mass loss up to 325 °C, which is much higher than its melting point (152 °C).)

dilution. Moreover, the NOESY intensities between the aromatic protons in the ROESY spectrum further affirms the presence of intermolecular hydrogen bonding between the aromatic protons (Fig. 8).

Absorption studies

Owing to the ecofriendly nature of peptides, they are considered to be attractive targets for the design of nanoporous materials.[18] Inspired by the guest molecule adsorption properties in the architecture of a double helix,[19] the author aims to explore the candidature of the enantiomeric pseudopeptides in the design of nanoporous materials. Since enantiomers exhibit identical properties, only one of the enantiomers (pseudopeptide **II**) was subjected to guest molecule encapsulation studies.

The TGA experiments of pseudopeptide **II** reveal that the supramolecular double helices have significant thermal stability. It showed no decomposition, phase transitions or mass loss up to 325 °C, which is much higher than the melting point (Fig. 9).

The exposure of the sample was carried out in a closed chamber for 24 h, where iodine vapours were generated by warming the chamber at regular time intervals.[20] It was observed that colorless crystals of pseudopeptide **II** turned dark brown (Fig. 10) (Table 4) (9.7 wt%). The crystals of pseudopeptide **II** after iodine absorption were not suitable for diffraction so we are unable to comment on the cell parameters of the iodine absorbed crystals. To verify the

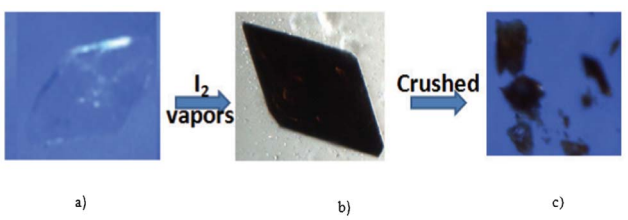

Fig. 10 Photograph of a) a single crystal of pseudopeptide **II**; b) after exposure to iodine vapours; c) showing the uniform absorption of iodine vapours in the crystal after crushing.

Table 4 Initial weight of the sample = 41.4 mg. Weight loss of the I_2 exposed sample of pseudopeptide **II** in air

Time (min)	Wt of the sample (mg)	Wt increase (mg)	% Wt increased
0	45.70	4.30	10.4
10	41.56	4.14	10.1
20	37.47	4.09	9.9
30	33.38	4.01	9.7
40	33.38	4.01	9.7
50	33.38	4.01	9.7
60	33.38	4.01	9.7
120	33.38	4.01	9.7
180	33.38	4.01	9.7
24 hours	33. 38	4.01	9.7

nature of the absorption, the crystals of pseudopeptide **II** after iodine exposure were crushed. The color inside the crystals was found to be dark brown for pseudopeptide **II**, indicating uniform absorption (Fig. 10). To affirm our results, further surface area measurement studies were performed.[21] The evacuated samples of pseudopeptide **II** indicate that they exhibit a type-III absorption isotherm (Fig. 11). The pore size distribution curve of pseudopeptide **II** showed a peak maxima at 1.88 nm at 77 K and 1 atm pressure.

Conclusions

In summary, this report reflects that in the solid state, two enantiomeric pseudopeptides **I** and **II**, comprising a single pyridinedicarboxylic acid and a flexible dipeptidyl fragment H-Xaa-*m*ABA-OMe (Xaa: L-Ala, pseudopeptide **I**; D-Ala, pseudopeptide **II**, *m*ABA: *meta* aminobenzoic acid), displays supramolecular double helical assemblage by employing dimeric

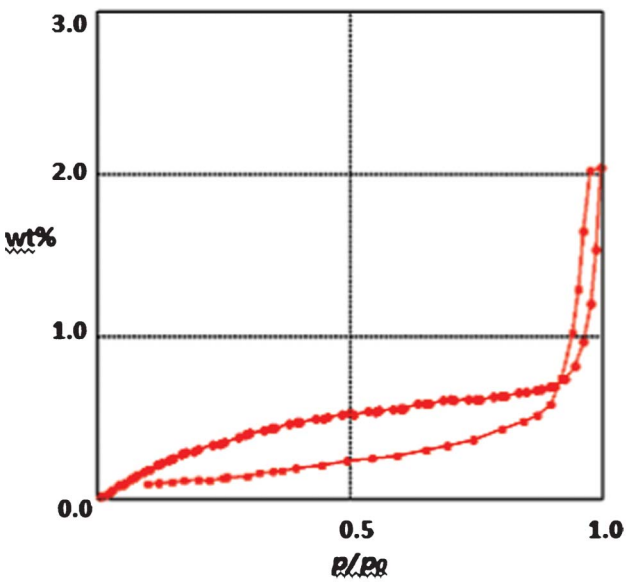

Fig. 11 N_2 adsorption–desorption isotherm of pseudopeptide **II** at 77 K and 1 atm pressure. Red square: sorption; red circle: desorption.

subunits as building blocks. To date, significant examples are documented in the literature where DNA analogues/derivatives or several rigid templates have been employed as synthons for double helical self assembly. However, to the best of our knowledge, this novel example represents one of the very few reports of supramolecular double helix design resulting from the self assembly of a flexible dimeric peptidyl unit, solely nucleated by the conformational features, of the peptides and stabilized by non-covalent interactions (H-bonding and π–π interactions) as the driving force. Concentration and temperature dependant NMR experiments and ESI-MS analysis also supported the existence of the dimeric unit in solution of pseudopeptide **I** (one of the enantiomers). Pseudopeptide **II** (one of the enantiomers) was subjected to iodine and gas absorption studies, which demonstrates their candidature in the design of nanoporous materials.

This report further reveals that careful engineering of flexible amino acid/peptidyl fragments coupled with a single pyridinedicarboxylic acid for the design of supramolecular double helical assemblage with large pore diameters, to display successful adsorption properties, is currently under investigation. This path may open a new avenue for scientists to tailor environmentally benign peptide based nanoporous materials.

Acknowledgements

The author wishes to thank DST, New Delhi, India, for financial support (Project No. SR/FT/CS-025/2010) and IISER Bhopal for providing the infrastructures. The author is very grateful to Dr. Sanjit Konar for their assistance in the X-ray crystallography and valuable advice. Mr. Amit Adhikary, Mr. Javeed Ahmad Sheikh, Mr. Suresh Sanda, Mr. Soumyabrata Goswami, Mr Sajal Khatua, Mr. Soumava Biswas and Mr. P. Sreenivasulu are sincerely acknowledged for various measurements for this work.

References

1 (*a*) M. M. Cox and D. L. Nelson, *Principles of Biochemistry*, W. H. Freeman and Company, New York, 2008; (*b*) A. Bruce, *Molecular Biology of the Cell*, Garland Science, New York, 2008.
2 J. D. Watson and F. C. H. Crick, *Nature*, 1953, **171**, 737.
3 (*a*) B. Petersson, B. B. Nielsen, H. Rasmussen, I. K. Larsen, M. Gajhede, P. E. Neilsen and J. S. Kastrup, *J. Am. Chem. Soc.*, 2005, **127**, 1424; (*b*) R. W. Wanger, *Nature*, 1994, **372**, 333; (*c*) M. Egli, P. S. Pallan, R. Pattanayek, C. J. Wilds, P. Lubini, G. Minasov, M. Dobler, C. J. Leuman and A. Eschenmoser, *J. Am. Chem. Soc.*, 2006, **128**, 10847; (*d*) M. Tarkoy and C. Leumann, *Angew. Chem., Int. Ed.*, 1993, **32**, 1432.
4 (*a*) A. D. Konar, *CrystEngComm*, 2012, **14**, 6689; (*b*) C. H. Gorbitz, *Chem.–Eur. J.*, 2007, **13**, 1022; (*c*) S. Guha, M. G. B. Drew and A. Banerjee, *Org. Lett.*, 2007, **9**, 1347; (*d*) P. Jana, S. Maity, S. K. Maity and D. Haldar, *Chem. Commun.*, 2011, **47**, 2092; (*e*) S. K. Maity, S. Maity, P. Jana and D. Haldar, *Chem. Commun.*, 2012, **48**, 711.
5 (*a*) Y. Tanaka, H. Katagiri, Y. Furusho and E. Yashima, *Angew. Chem., Int. Ed.*, 2005, **44**, 3867; (*b*) Y. Furusho, Y. Tanaka and E. Yashima, *Org. Lett.*, 2006, **8**, 2583.
6 H. Goto, H. Katagiri, Y. Furusho and E. Yashima, *J. Am. Chem. Soc.*, 2006, **128**, 7176.
7 T. Sugimoto, T. Suzuki, S. Shinkai and K. Sada, *J. Am. Chem. Soc.*, 2007, **129**, 270.
8 G. J. Gabriel and B. L. Iversion, *J. Am. Chem. Soc.*, 2002, **124**, 15174.
9 (*a*) J. Li, J. A. Wisner and M. C. Jennings, *Org. Lett.*, 2007, **9**, 3267; (*b*) H. Bo, B. P. Mudraboyina, J. Li and J. A. Wisner, *Chem. Commun.*, 2010, **46**, 7343; (*c*) H. B. Wang, B. P. Mudraboyina and J. A. Wisner, *Chem.–Eur. J.*, 2012, **18**, 1322.
10 (*a*) V. Berl, I. Huc, R. G. Khoury, M. J. Krische and J. M. Lehn, *Nature*, 2000, **407**, 720; (*b*) E. Kolomiets, V. Berl and J. M. Lehn, *Chem.–Eur. J.*, 2007, **13**, 5466.
11 (*a*) D. Haldar, H. Jiang, J. A. Leger and I. Huc, *Angew. Chem., Int. Ed.*, 2006, **45**, 5483; (*b*) B. Baptiste, J. Zhu, D. Haldar, B. Kauffmann, J. M. Leger and I. Huc, *Chem.–Asian J.*, 2010, **5**, 1364; (*c*) H. Jiang, J. M. Leger and I. Huc, *J. Am. Chem. Soc.*, 2003, **125**, 3448; (*d*) Q. Gan, Y. Ferrand, C. Bao, B. Kauffmann, A. Grilard, H. Jiang and I. Huc, *Science*, 2011, **331**, 1172; (*e*) A. M. Kendhale, L. Poniman, Z. Dong, K. L. Reddy, B. Kauffmann, Y. Ferrand and I. Huc, *J. Org. Chem.*, 2011, **76**, 195.
12 (*a*) A. Dutt, M. G. B. Drew and A. Pramanik, *Org. Biomol. Chem.*, 2005, 2250; (*b*) S. K. Kundu, P. A. Mazumdar, A. K. Das, V. Bertolasi and A. Pramanik, *J. Chem. Soc., Perkin Trans.*, 2002, 1602; (*c*) P. Koley and A. Pramanik, *Soft Matter*, 2012, **8**, 5364; (*d*) P. Koley and A. Pramanik, *Adv. Funct. Mater.*, 2011, **21**, 4126.
13 M. Bodanszky and A. Bodanszky, *The Practice of Peptide Synthesis*, Springer-Verlag, New York, 1984, p. 1.
14 SADABS, G. M. Sheldrick, *Program for Absorption Correction of Area Detector Frames*, BRUKER AXS Inc., 5465 East Cheryl Parkway, Madison, WI 53711- USA.
15 (*a*) G. M. Sheldrick, *Acta Crystallogr., Sect. A: Fundam. Crystallogr.*, 1990, **46**, 467; (*b*) G. M. Sheldrick, SHELXL 97 *Program for Crystal Structure Refinement*, University of Göttingen, Germany, 1997.
16 D. Haldar, H. Jiang, J. M. Leger and I. Huc, *Tetrahedron*, 2007, **63**, 6322.
17 K. Wuthrich, in *NMR of Proteins and Nucleic Acids*, Wiley: New York, 1986, p. 192.
18 (*a*) C. H. Görbitz, *Chem.–Eur. J.*, 2007, **13**, 1022; (*b*) C. H. Görbitz, M. Nilsen, K. Szeto and L. W. Tangen, *Chem. Commun.*, 2005, 4288; (*c*) C. H. Görbitz, *CrystEngComm*, 2005, **7**, 670.
19 P. Jana, S. Maity, S. K. Maity and D. Haldar, *Chem. Commun.*, 2011, **47**, 2092.
20 (*a*) L. Dobrzanska, G. O. Lloyd, H. G. Raubenheimer and L. J. Barbour, *J. Am. Chem. Soc.*, 2005, **127**, 2937; (*b*) L. Rajput, V. V. Chernyshev and K. Biradha, *Chem. Commun.*, 2010, **46**, 6530.
21 D. Chandra and A. Bhaumik, *J. Mater. Chem.*, 2009, **19**, 1901.